Title: Evidence for habitual climbing in a middle Pleistocene hominin in South Africa

Authors: Leoni Georgiou[1], Christopher J. Dunmore[1], Ameline Bardo[1], Laura T. Buck[2], Jean-Jacques Hublin[3], Dieter H. Pahr[4,5], Dominic Stratford[6], Alexander Synek[4], Tracy L. Kivell[1,3,7], Matthew M. Skinner[1,3,7]

[1] Skeletal Biology Research Centre, School of Anthropology and Conservation, University of Kent, Canterbury, UK

[2] Department of Anthropology, University of California, Davis, California, USA

[3] Department of Human Evolution, Max Planck Institute for Evolutionary Anthropology, Leipzig, Germany

[4] Institute for Lightweight Design and Structural Biomechanics, Vienna University of Technology, Vienna, Austria

[5] Department of Anatomy and Biomechanics, Karl Landsteiner Private University of Health Sciences, Krems an der Donau, Austria

[6] School of Geography, Archaeology and Environmental Studies, University of the Witwatersrand, Johannesburg, South Africa

[7] Evolutionary Studies Institute, University of Witwatersrand, Johannesburg, South Africa

***Corresponding author:**

Dr Leoni Georgiou

School of Anthropology & Conservation

University of Kent

Canterbury, Kent CT2 8HA

United Kingdom

email: lg400@kent.ac.uk

Abstract

Bipedalism is a defining trait of the hominin lineage, associated with a transition from a more arboreal to a more terrestrial environment. While there is debate about when modern human-like bipedalism first appeared in hominins, all known South African hominins show morphological adaptations to bipedalism, suggesting that this was their predominant mode of locomotion. Here we present evidence that hominins preserved in the Sterkfontein Caves practised two different locomotor repertoires. The trabecular structure of a proximal femur (StW 522) attributed to *Australopithecus africanus* exhibits a modern human-like bipedal locomotor pattern, while that of a geologically-younger specimen (StW 311) attributed to either *Homo* sp. or *Paranthropus robustus* exhibits a pattern more similar to non-human apes, potentially suggesting regular bouts of both climbing and terrestrial bipedalism. Our results demonstrate distinct behavioural differences between *Australopithecus* and later hominins in South Africa and contribute to the increasing evidence of locomotor diversity within the hominin clade.

Significance Statement

Here we present new evidence of hominin locomotor behaviour from the trabecular bone structure of the femur. We show evidence for habitual use of highly flexed hip postures, which could potentially indicate climbing in a South African hominin from Sterkfontein, which is either *Paranthropus robustus* or *Homo*. Second, we present evidence that *Australopithecus africanus* likely did not climb at the frequencies seen in extant non-human apes, and exhibits a modern, human-like pattern of loading at the hip joint. These results challenge the prevailing view of a single transition to bipedalism within the hominin clade by

providing evidence of climbing in a more recent, non-*Australopithecus* South African hominin, and add to the increasing evidence for locomotor diversity in the hominin clade.

Introduction

Skeletal adaptations for bipedal locomotion in the hominin lineage date back to at least six million years ago[1]. These bipedal adaptations are found throughout the skeleton, but those of the hip and knee are particularly important as these joints are central in determining how load is transferred through the lower limb. In modern humans, femoral adaptations for bipedalism include a relatively large femoral head, long neck[2] and a high bicondylar angle compared with extant apes, as well as flat, ellipsoid distal condyles and an elevated patellar lip[3,4]. Conversely, in African apes the femoral head is relatively small and the neck short[2], while the distal condyles are more circular[3,4]. Identifying bipedal adaptations in fossil apes is critical to placing them on the hominin lineage, however the presence of such adaptations in the earliest fossil hominins (e.g. *Sahelanthropus*, *Orrorin* and *Ardipithecus*) is controversial[1,5,6]. Generally accepted evidence for obligate bipedalism is found in later hominins, such as the australopiths[7-9]. Here we test for evidence of committed terrestrial bipedalism and/or evidence for significant bouts of climbing in South African hominins, including *Australopithecus africanus*.

Adaptations for bipedalism appear in the tibia of the earliest known australopith, *Australopithecus anamensis*[9], however the absence of additional lower limb postcranial remains belonging to this taxon limits the interpretation of its locomotion. The more complete fossil record for *Australopithecus afarensis* includes femoral specimens with a long femoral neck and human-like femoral muscular organisation in the proximal femur[10] as well

as a raised patellar lip, ellipsoid condyles and a deep patellar groove in the distal femur[4] suggesting that they frequently adopted bipedality. Similar traits are found in *Australopithecus africanus*[3]. Furthermore, other South African fossils, including *Australopithecus sediba*[11] and *Australopithecus* sp. StW 573[12,13], strengthen this notion that australopiths were committed terrestrial bipeds. However, the different mosaics of human- and ape-like external traits in australopiths have led to debate over the form of bipedalism[14,15], as well as the levels of arboreality in these taxa[16,17]. More definitive traits for mechanically modern human-like, obligate bipedalism appear in *Homo erectus* and most later *Homo* taxa[18-20], but the locomotion of other *Homo* taxa, including *Homo habilis*, is still poorly understood[21,22].

Most studies of fossil hominin bipedalism have focused on external morphological traits[1,4,13]. However, debates about behavioural interpretations based on external morphology have arisen due to the suggestion that, in the absence of strong selective pressure, primitive traits can be retained that are no longer functionally relevant[15]. Additionally, it has been argued that some Pliocene hominins may exhibit functional divergence of the upper and lower limbs associated with selection for both arboreality and terrestrial bipedalism, respectively[13,23].The discoveries of StW 573 (nicknamed 'Little Foot')[12,13], *A. sediba*[24], *Homo floresiensis*[25] and *Homo naledi*[26] reveal additional unexpected combinations of ape-like and human-like morphologies in the hominin fossil record. To better understand actual, rather than potential, behaviour in the past, this study focuses on reconstructing predominant joint positions habitually practiced by fossil hominin individuals through the analysis of internal bone structure (trabecular or cancellous bone) to clarify the locomotor repertoire in different species.

Investigation of trabecular architecture in long bones has proven integral in reconstructing behaviours in both extant and fossil humans, as well as other primates[27-31]. This is because trabecular bone responds to load via modelling and remodelling, mainly altering the orientation of its struts, as well as the distribution and volume of bone[32]. Analysis of trabecular architecture has revealed behavioural signals in the femoral head of primates [29,30,33]. Our previous work has shown that within the femoral head, trabecular bone distribution differs between humans, African apes and orangutans[30] and correlates with predicted pressure from habitual postures. Furthermore, within the femoral head, modern humans have highly aligned struts (expressed as high degree of anisotropy, or DA) and distinct strut orientation compared to other apes[29], traits that are consistent with obligate bipedalism. Bone volume fraction (expressed as bone volume/total volume or BV/TV) is significantly lower in modern humans relative to great apes, but varies with activity levels, with more sedentary modern humans showing lower bone volume within the femoral head than more active humans[31]. Trabecular studies in the femoral head[29] and distal tibia[27] of *A. africanus* have shown that the trabeculae are highly aligned and oriented in a similar manner to humans and distinct from chimpanzees. However, these studies focused on sub-volumes (or 2D slices) of trabecular bone and since trabecular structure is not homogeneously distributed across epiphyses[34], analysing isolated volumes may obscure or limit functional interpretations. In particular, recent studies have shown that the analysis of subchondral trabecular bone distribution and architecture is crucial to revealing differences in joint loading across primates that practice different locomotor repertoires[27,29,34].

Here we conduct a comparative analysis of the 3D trabecular bone distribution beneath the subchondral layer of the proximal femoral head in humans, other great apes and two fossil hominin specimens from the Sterkfontein Caves, South Africa (StW 311 and StW 522;

Supporting Figure 1; Supporting Figure 2A). StW 522 derives from Member 4 (See Supporting Information) which has been dated broadly to 2.8 to 2.0 Ma[35]. This specimen has been attributed to *A. africanus*[36]. The StW 311 proximal femur derives from the stratigraphically complex eastern end of Member 5 at Sterkfontein (named Member 5 East – M5E)[37], where two infills are recognised, both of which are artefact- and hominin-bearing. The lower infill unit, recently dated to 2.18 Ma[38], contains *P. robustus* remains and Oldowan artefacts. However, previously it has been suggested to date from 1.7-1.4 Ma[37] and 1.4-1.2 Ma[35]. The upper unit of M5E, dated to 1.7-1.4 Ma[37] or 1.3-1.1 Ma[35], is characterised by early Acheulean stone tools. Although StW 311 has been previously attributed to *A.* africanus[2,29], revision of the stratigraphy of this area of the Sterkfontein deposits suggests that this specimen derives from the M5E infill[37] and thus should be either attributed to early *Homo* or *P. robustus*. Unfortunately, this specimen does not preserve enough of the proximal epiphysis to be taxonomically diagnostic and thus its attribution remains uncertain. Finally, although StW 311 is larger in absolute size than StW 522 (Supporting Figure 2), both specimens show almost identical external morphology that has been previously interpreted indicative of habitual bipedal locomotion[3,29].

To investigate the potential locomotor signals within the trabecular structure of the Sterkfontein hominin femoral specimens, we combine geometric morphometrics with trabecular analysis of the whole epiphysis (Supporting Figure 3A) to quantify and compare bone volume fraction at homologous locations across extant and fossil taxa. Based on predictions from joint morphology, hindlimb postures and peak pressure data[39-43], we first investigate locomotor signals preserved in the trabecular structure of the femoral head of extant non-human great apes, including terrestrially knuckle-walking and arboreally climbing African apes (*Pan troglodytes verus* n=11, *Pan t. troglodytes* n=5, *Gorilla gorilla gorilla*

n=11) and orthograde arboreal orangutans (*Pongo* sp. n=5). We predict that great apes will show a trabecular distribution (i.e., concentrations of high BV/TV) that is consistent with loading of the femoral head in both extended and highly flexed hip postures (Figure 1), which occur during quadrupedalism, bipedalism and vertical climbing. Second, we investigate the trabecular pattern in recent *Homo sapiens* (n=11) and the femoral head of a fossil *H. sapiens* individual (Ohalo II H2). In contrast to great apes, we predict that recent and fossil *H. sapiens* and will show a trabecular distribution that is consistent with posterior loading of the femoral head due to hip-joint incongruency and the use of habitual, more extended hip postures during bipedalism (Figure 1).. Finally, we assess the trabecular bone distribution in the femoral heads of StW 311 and StW 522, to determine whether they show functional signals in the femur consistent with ape-like, human-like or distinct modes of locomotion. We predict that StW 522, attributed to *A. africanus*[36], will present a distinct trabecular pattern that shows similarities to both humans and great apes, given skeletal evidence suggesting that this taxon was a committed terrestrial biped that engaged in facultative arboreality[4,7,8]. Predictions for StW 311 are complicated by its taxonomic uncertainty and possible evidence for arboreality in *P. boisei*[44]. If StW 311 represents *Homo,* then we predict a more human-like pattern; however, if it represents *Paranthropus* (and if one expects some level of arboreality in all members of this genus) then we predict that, like StW 522, it will show similarities to both humans and great apes.

Locomotor signals within the proximal femur of non-human great apes

Variation in the distribution of subchondral trabecular bone in the femoral head of non-human great apes is consistent with our predictions based on inferred joint position and pressure distribution in the hip during terrestrial as well as arboreal locomotion (Figure 2;

Supporting Figure 4C; for average distribution maps for each taxon see Supporting Figure 3B; for trabecular architecture results see Supporting Table 1 and for intertaxon comparisons of mean trabecular values see Supporting Table 2). Extant non-human apes show two concentrations of high BV/TV across the surface of the femoral head (Figure 2B; Supporting Figure 3B) that extend internally as two converging "pillars" or in the formation of an inverted cone (Figure 2C; Supporting Figure 5). *Gorilla* has the most consistently well-separated regions of high BV/TV, followed by *Pan*, while *Pongo* that has the least separated concentrations. The anterior concentration in all non-human apes is consistent with the presumed region of high pressure when hips are highly flexed during vertical climbing[39], while the posterior concentration is consistent with the region of high pressure when hips are more extended during terrestrial locomotion[40] (Figures 1, 2A; Supporting Figure 4C). Compared with *Gorilla*, there is a more expansive distribution in *Pan* and *Pongo* of high BV/TV across the superior aspect of the head indicating a more variable pattern of joint positioning and pressure distribution. This is consistent with the use of more varied hip flexion angles during arboreal locomotion when needing to navigate complex forest canopies[41]. The more restricted areas of BV/TV concentration in *Gorilla* suggest a more dichotomous joint positioning pattern, perhaps associated with reduced arboreality and/or large body size[39,45].

***Locomotor signals in recent and fossil* Homo sapiens**

The pattern found in the femoral head of recent *H. sapiens* and Ohalo II H2 is distinct from that of other great apes, showing one region of high BV/TV located posteriorly and medially on the femoral head (Figure 3; Supporting Figure 3B). The region of high BV/TV corresponds to the region of highest pressure during a bipedal gait (Figure 1; Supporting

Figure 4B)[42]. Additionally, the extended range of intermediate values across the head is consistent with hip loading from positions of moderate flexion towards moderate extension[46]. Intermediate BV/TV values continue along the inferior aspect of the femoral head (Supporting Figure 4B). Internally, *H. sapiens* shows the distinct feature of a single pillar of high BV/TV extending beneath the posterior-superior concentration towards the femoral neck (Figure 3C; Supporting Figure 5).

Trabecular distribution patterns and locomotor reconstruction of Sterkfontein hominins

The two proximal femur fossil specimens from Sterkfontein show different trabecular patterns. The femoral head of StW 522 (attributed to *A. africanus*) exhibits one high BV/TV concentration along the superior aspect of the femoral head, located medially and close to the fovea capitis, that extends internally as a single pillar (Figure 4; Supporting Figures 3C,5). This pattern, as well as the intermediate BV/TV values that continue across the inferior aspect of the femoral head, resembles that of *H. sapiens*. Despite the high BV/TV concentration being located slightly more anteriorly and mean femoral head trabecular parameters (e.g., DA, trabecular number and thickness) falling within the extant ape range (Supporting Figure 2B), the BV/TV distribution pattern of this specimen is almost identical to *H. sapiens*. Contrary to single trabecular parameters[33], BV/TV distribution patterns in the femur[30] and other bones[28,34], have been shown to distinguish between great apes with different locomotor repertoires, therefore these results suggest that StW 522 used a similar bipedal gait to *H. sapiens*.

In contrast to StW 522, the geologically younger proximal femur StW 311 shows a more ape-like trabecular pattern. This individual has two concentrations of high BV/TV along the

superior aspect of the femoral head that extend internally towards the neck (Figure 4). The ape-like anterior concentration suggests that, in addition to typical bipedalism, this individual frequently adopted a highly flexed hip posture. Furthermore, in contrast to previous findings[29], mean femoral head trabecular parameters of StW 311 fall consistently within the *Pan* range (Supporting Figure 2B). Although these mean values may obscure or homogenise the variation in each trabecular parameter within the femoral head, our results show that StW 311 has low anisotropy and high BV/TV compared to the typical pattern in sedentary *H. sapiens*[29].

To further assess the trabecular architecture of the Sterkfontein femoral specimens compared to extant apes and recent and fossil *H. sapiens*, we conducted an analysis of relative BV/TV (RBV/TV) distribution in the femoral head using geometric morphometric techniques. Two hundred and forty-two landmarks and semilandmarks were defined on the subchondral femoral head. Subsequently, BV/TV values were extracted at each subchondral landmark and were standardised by the mean BV/TV value of all subchondral landmarks extracted from that specimen, resulting in a relative bone volume fraction (RBV/TV). RBV/TV values were then statistically compared between taxa, to identify relative differences in their distributions, rather than raw of trabecular volume values. Figure 5 presents a principal component (PC) analysis of the landmark-based RBV/TV distribution in the femoral head of all taxa. Consistent with the overall patterns described above for the extant taxa, along PC1 *Gorilla* is distinguished from *Pan* and *Pongo* species, which cluster together, while *H. sapiens* is clearly separated from all other apes. Permutational MANOVA tests of the first three principal components reveal that the distributions of all taxa differ significantly, except that of *Pan t. troglodytes* from the other non-human apes (Supporting Table 3). Ohalo II H2 falls just outside the recent human distribution but shows the same subchondral trabecular pattern.

This is consistent with the fact that our *H. sapiens* sample does not include sufficient variation in terms of geographic distribution and behavioural diversity. Both StW 522 and StW 311 fall out as intermediate between *H. sapiens* and *Pan*/*Pongo*, but StW 311 is closer to the non-human apes. This result reflects the quantification of only the subchondral trabecular bone (i.e. it does not quantify the distinct internal BV/TV structure throughout the femoral head between StW 311 and StW 522), in which the trabecular distribution of StW 522 shows one high BV/TV concentration that is located slightly more anteriorly than that of humans, while StW 311 shows two regions of high BV/TV.

Discussion

In this study, we demonstrate that known differences in the locomotor behaviour of non-human apes and humans are reflected in the trabecular structure of the femur. We also provide the first substantive evidence that early Pleistocene fossil hominins from Sterkfontein, who existed at different times, were using distinct forms of locomotor behaviour. Contrary to our predictions, *A. africanus* StW 522 showed a distinctly human-like trabecular bone distribution. This result reveals that this individual was likely an obligate biped, in accordance with prior *Australopithecus* findings[9,13] and the more human-like external morphology of the pelvis and knee of *A. africanus*[4,7,8]. Importantly, the StW 522 trabecular pattern suggests that the more ape-like features typical of *Australopithecus* skeletons[11-13] are likely evolutionary retentions rather than evidence for frequent climbing. If the trabecular bone is adequately imageable, analyses of the near complete skeleton of *Australopithecus* sp. StW 573[13] (‘Little Foot’) may further elucidate the locomotor behaviour of Sterkfontein hominins.

Given the similar external morphology between the Sterkfontein proximal femora in our sample, trabecular evidence that StW 311 frequently used highly flexed hip postures typical of climbing is unexpected. This result is consistent with paleoenvironmental reconstructions from faunal evidence[47] that suggest that there was significant tree coverage near the Sterkfontein caves during the accumulation of the Member 5 East infill, but drier climate than Member 4 (see Supporting Information). However, as is common in vertebrate palaeontology, it is difficult to place individuals in a particular part of a diverse landscape. There are various ways in which StW 311 may have come to be preserved at Sterkfontein, including carnivore accumulation, water transport, or death traps[47,]. Thus, although a climbing signal is most often associated with arboreality in a wooded environment, climbing within a karstic environment is also a possibility. Additionally, it is uncertain if other highly flexed-hip behaviours, such as frequent squatting, could result in a similar trabecular distribution pattern to that of climbing in apes. This could be explored in human samples with evidence for squatting in the lower limb bones (e.g., squatting facets[48]). However, our expectation is that positional loading during squatting is unlikely to result in comparisons between human groups resembling the dichotomous pattern we find between humans and non-human apes.

Our results from the trabecular analysis of StW 311 add to those previously described in a distal tibia specimen (StW 567) from the Member 5 East infill. Barak and colleagues[27] found that this individual had human-like trabecular orientation, that differs from chimpanzees, reflecting the use of a less dorsiflexed ankles. However, the mean trabecular parameters of this specimen were not distinctly human-like. For example, BV/TV in the two studied volumes of interest of StW 567 was higher than both *H. sapiens* and *P. troglodytes*, DA was more similar to *P. troglodytes*, and trabecular number, separation and connectivity were

intermediate between the two extant taxa. The lack of certainty on the taxonomic affinity of StW 567 introduces difficulties in the interpretation of these results, as we do not know if it belongs to the same taxon as StW 311 and the Member 5 East infill contains both *P. robustus* and early *Homo* fossils. An associated lower limb that included both the femur and tibia may elucidate the likelihood that these two specimens could sample the same taxon.

Based on our predictions, evidence for the frequent use of a highly flexed hip joint in the StW 311 individual could be evidence in support of this specimen belonging to *Paranthropus*, rather than *Homo*. However, there are a number of important points that must be considered. First, evidence for arboreality in *Paranthropus boisei* is limited to a scapula, which shows both arboreal and non-arboreal features[44], a distal humerus[49], and a proximal radius[50]. Additionally, there is no direct evidence for a shared locomotor repertoire between eastern and southern African *Paranthropus* species (as well as debate about the monophyletic nature of the genus). Second, postcranial signals of arboreality have been noted in some early *Homo* specimens, such as OH 62[19], and it is thus conceivable for StW 311 to both represent *Homo* and show evidence for arboreality. Finally, two proximal femora from Swartkrans (SK 3121 and SKW 19), which could also be either *P. robustus* or early *Homo*, were not included in this study due to poor preservation of the femoral head articular surface (Supporting Figure 6). However, there is potential evidence from the internal BV/TV distribution (Supplementary Figure 7B) for a human-like single concentration in these specimens. Determining the taxonomic affiliation of not only StW 311, but also SK 3121 and SKW19 remains crucial as it will have clear implications, and perhaps explanations, for niche differentiation between these two genera who differ in gnathic morphology, but less so in dental microwear and dietary isotopic data[51].

Finally, the results of this study add to the increasing evidence for locomotor diversity in the Plio-Pleistocene hominin record including a mix of primitive and derived features in 'Little Foot'[13], *A. sediba*[24] and *H. naledi*[26], the abducted hallux in the Burtele foot[52], and more ape-like than hominin-like lower limb morphology in *Ardipithecus ramidus*[5]. We suggest that future studies of internal bone structure (both cortical distribution and trabecular architecture) will be crucial to clarifying the diversity of locomotor behaviours that characterized various hominin lineages.

Materials and Methods

Sample, segmentation and trabecular architecture analysis

In this study we used micro-computed tomographic scans to analyse trabecular architecture in the femoral head of five extant ape taxa (*Pan troglodytes verus* n=11, *Pan troglodytes troglodytes* n=5, *Pongo* sp. n=5, *Gorilla gorilla* n=11 and *H. sapiens* n=10) and three fossil specimens (StW 311, StW 522 and Ohalo II H2), detailed in Supporting Table 4. The *Pan troglodytes verus* individuals came from the Taï forest, while four of the *P.t.troglodytes* individuals came from Gabon and one from Cameroon. We included two sub-species of *Pan* to show the sensitivity of our method in detecting differences in BV/TV distribution between closely related taxa with few behavioural differences. All *Gorilla* individuals were western lowland gorillas, and thirteen came from Cameroon while one came from the Democratic Republic of the Congo. The *Pongo* sample consisted of one *Pongo abelii* individual, three *Pongo pygmaeus* individuals and one unspecified. All non-human apes were wildshot. The *Homo sapiens* individuals came from two 19th-20th century cemeteries in Germany. Several South African hominin specimens (e.g. SK 3121, SKW 19, SK 82, SK 97) were excluded

from our analysis because of difficulties in obtaining an accurate representation of the trabecular structure or limited preservation that excluded homologous landmarking (Supporting Figures 6,7). All individuals were adult and showed no signs of pathologies. Prior to analysis, all specimens were re-oriented to approximate anatomical positions, as well as cropped and re-sampled when necessary using AVIZO 6.3 ® (Visualization Sciences Group, SAS).

Segmentation of bone from air was performed using the Ray Casting Algorithm[53] for the extant sample and the MIA-clustering algorithm[54] for the fossil sample. The latter was used for fossils as it allows more accurate separation of trabecular bone from surrounding inclusions. Trabecular architecture was analysed in medtool 4.1 (www.medtool.at), following previously described protocol[55]. Three-dimensional tetrahedral meshes with a 1mm mesh size were created using CGAL 4.4 (CGAL, Computational Geometry, http://www.cgal.org) and BV/TV values, which were obtained using a sampling sphere with a 7.5mm diameter, on a 3.5mm background grid, were interpolated onto the elements creating BV/TV distribution maps. Internal BV/TV distribution was visualised in Paraview[56] above selected percentiles which were calculated for each femoral head using the quantile function in R v3.4.1[57]. The visualisation shows where the highest 15%, 20% and 25% of the BV/TV values lie within that femoral head (Supporting Figure 5). This method was chosen to ensure that the selected thresholds were not affected by outliers and that isolated patterns were comparable between specimens.

The subchondral surface of the resulting 3D models was extracted and smoothed using Screened Poisson surface reconstruction in MeshLab[58] in preparation for landmarking.

376 *Landmarking and BV/TV values extraction*

377

378 Initially, fixed landmarks were selected for the femoral head. Intra-observer error for the
379 fixed landmarks was tested by placing the landmarks on 3 specimens of the same taxon at 10
380 non-consecutive occasions. Five fixed landmarks were identified on the femoral head; one
381 point in each direction of the head-neck border (most anterior, most posterior, most lateral
382 and most medial) at the midpoint and one on the surface of the femoral head, at the centre of
383 the four corner landmarks (Supporting Figure 3A). Four semi-curves were defined between
384 the fixed landmarks along the femoral head-neck boundary, each containing 7 landmarks.
385 Subsequently, two hundred and eight semilandmarks[59] were defined on the surface of the
386 femoral head. These were evenly spaced landmarks extending across the whole femoral
387 articular surface. Thirty-two of the semilandmarks were placed between the fixed landmarks
388 on the head-neck boundary (1-4) and the 5th landmark at the midpoint of the corner
389 landmarks, thus dividing the femoral head into quarters. The remaining landmarks were
390 placed covering the surface of the quarters. Further description of the landmarks is given in
391 Supporting Table 5.

392

393 The fixed and curve landmarks were manually defined on all specimens, while the surface
394 semilandmarks were defined on one specimen and then projected on all other specimens
395 using the Morpho package[60] in R v3.4.1[57]. After manual inspection of the projected
396 landmarks on each specimen, the landmarks were relaxed on the surface minimising bending
397 energy. Subsequently, the Morpho package was used to slide the surface and curve landmarks
398 minimising Procrustes distance. A medtool 4.1 custom script was used to interpolate BV/TV
399 values to landmark coordinates from the closest neighbouring tetrahedron in distribution
400 maps of each specimen. Relative BV/TV (RBV/TV) values were calculated for each

landmark by dividing landmark BV/TV values by the average of all BV/TV landmark values of each individual. Relative values were used for the statistical analysis to ensure inter-taxon comparisons focused on differences in the distribution rather than magnitude.

Statistical analysis

Statistical analysis was performed in R v3.4.1[57]. A principal components (PC) analysis was used to visualise interspecific differences in RBV/TV distributions. To exemplify the sensitivity of this method we evaluated the distributions of the *Pan* subspecies separately. Bonferroni-corrected, one-way pairwise permutational MANOVA tests of the first three principal components were used to test whether observed differences between the taxa in the PCA are significant. The three first components were chosen as they explained high percentages of the variation and together amounted to more than ~50%.

Acknowledgements: We thank the following researchers for access to specimens in their care: Anneke Van Heteren (Zoologische Staatssammlung München), Brigit Grosskopf (Georg-August University of Goettingen), Christophe Boesch (Max Planck Institute for Evolutionary Anthropology), and Inbal Livne (Powell-Cottom Museum). We also thank Keturah Smithson (University of Cambridge) and David Plotzki (Max Planck Institute for Evolutionary Anthropology) for the CT scanning of specimens**.** We also thank two anonymous reviewers for helping improve this manuscript. **Funding:** This research is supported by a 50th Anniversary Research Scholarship, University of Kent (L.G.), European Research Council Starting Grant 336301 (M.M.S., T.L.K.), The Fyssen Foundation (A.B.) and the Max Planck Society (M.M.S., T.L.K., J-J. H.). **Author contributions:** L.G. contributed to the design of the experiments, the acquisition, analysis and interpretation of

data, as well as drafted and substantially revised the manuscript, T.L.K contributed to the design of the experiments, the interpretation of data and the revision of the manuscript, A.B. contributed to the analysis and interpretation of data, as well as the revision of the manuscript, L.T.B. contributed to the acquisition and interpretation of data, as well as the revision of the manuscript, C.J.D. contributed to the analysis and interpretation of data, as well as the revision of the manuscript, J-J.H. contributed to the acquisition of data and the revision of the manuscript, D.H.P. contributed to the creation of the software used in this work, to the interpretation of data and the revision of the manuscript, D.S. contributed to the interpretation of data and the revision of the manuscript, A.S. contributed to the interpretation of data and the revision of the manuscript, M.M.S. contributed to the design of the experiments, the interpretation of data and the revision of the manuscript. All authors have approved the submitted version. **Competing interests:** The authors declare no conflicts of interest. **Data and materials availability:** https://doi.org/10.5061/dryad.ngf1vhhqd.

References

1. S. Almécija, M. Tallman, D. M. Alba, M. Pina, S. Moyà-Solà, W. L. Jungers, The femur of *Orrorin tugenensis* exhibits morphometric affinities with both Miocene apes and later hominins. *Nature Communications*, **4**, 2888 (2013).
2. E. H. Harmon, The shape of the early hominin proximal femur. *American Journal of Physical Anthropology*, **139**, 154-171 (2009).
3. K. G. Heiple, C. O. Lovejoy, The distal femoral anatomy of *Australopithecus*. *American Journal of Physical Anthropology*, **35**, 75–84 (1971).
4. C. Tardieu, 'Morpho-functional analysis of the articular surface of the knee joint in primates', in Chiarelli A., Corruccini R. (eds). *Primate evolutionary biology*. New York: Springer-Verlag, 68-80 (1981).

5. C. O. Lovejoy, G. Suwa, S. W. Simpson, J. H. Matternes, T. D. White, The great divides: *Ardipithecus ramidus* reveals the postcrania of our last common ancestors with African apes. *Science*, **326**, 73-106 (2009).
6. M. H. Wolpoff, B. Senut, M. Pickford, J. Hawks, *Sahelanthropus* or *'Sahelpithecus'*? *Nature*, **419**, 581-582 (2002).
7. R. Broom, J. T. Robinson, Further Remains of the Sterkfontein Ape-Man, *Plesianthropus*. *Nature*, **160**, 430-431 (1947).
8. J. R. Napier, The evolution of bipedal walking in the hominids. *Archives of Biology (Liege)*, **75**, 673-708 (1964).
9. C. V. Ward, M. G. Leakey, A. Walker, The new hominid species *Australopithecus anamensis*. *Evolutionary Anthropology: Issues, News, and Reviews*, **7**, 197-205 (1999).
10. C. O. Lovejoy, The natural history of human gait and posture: Part 2. Hip and thigh. *Gait & posture* **21**, 113-124 (2005).
11. J. M. DeSilva, K. G. Holt, S. E. Churchill, K. J. Carlson, C. S. Walker, B. Zipfel, L. R. Berger, The lower limb and mechanics of walking in *Australopithecus sediba*. *Science*, **340**, 6129 (2013).
12. R. J. Clarke, Excavation, reconstruction and taphonomy of the StW 573 *Australopithecus prometheus* skeleton from Sterkfontein Caves, South Africa. *Journal of Human Evolution*, **127**, 41-53 (2019).
13. J. Heaton, T. R. Pickering, K. J. Carlson, R. H. Crompton, T. Jashashvili, A. Beaudet, L. Bruxelles, K. Kuman, A. J. Heile, D. Stratford, R. J. Clarke, The long limb bones of the StW 573 *Australopithecus* skeleton from Sterkfontein Member 2: Descriptions and proportions. *Journal of Human Evolution*, **133**, 167-197 (2019).

14. J. T Jr. Stern, R. L. Susman, The locomotor anatomy of *Australopithecus afarensis*. *American Journal of Physical Anthropology,* **60**, 279-317 (1983).
15. C. O. Lovejoy, M. A. McCollum, Spinopelvic pathways to bipedality: why no hominids ever relied on a bent-hip–bent-knee gait. *Philosophical Transactions of the Royal Society of London B: Biological Sciences*, **365**, 3289-3299 (2010).
16. C. V. Ward, Interpreting the posture and locomotion of *Australopithecus afarensis*: where do we stand? *Yearbook of Physical Anthropology*, **45**, 185-215 (2002).
17. J. Kappelman, R. A. Ketcham, S. Pearce, L. Todd, W. Akins, M. W. Colbert, M. Feseha, J. A. Maisano, A. Witzel, Perimortem fractures in Lucy suggest mortality from fall out of tall tree. *Nature,* **537**, 503 (2016).
18. E. Trinkaus, Functional aspects of Neanderthal pedal remains. *Foot Ankle*, **3**, 377-390 (1983).
19. C. B. Ruff, Relative limb strength and locomotion in *Homo habilis*. *American Journal of Physical Anthropology*, **138**, 90-100 (2009).
20. K. G. Hatala, N. T. Roach, K. R. Ostrofsky, R. E. Wunderlich, H. L. Dingwall, B. A. Villmoare, D. J. Green, J. W. K. Harris, D. R. Braun, B. G. Richmond, Footprints reveal direct evidence of group behavior and locomotion in *Homo erectus*. *Scientific Reports*, **6**, 28766 (2016).
21. M. H. Day, J. R. Napier, Fossil foot bones from Olduvai Gorge. *Nature*, **201**, 969-970 (1964).
22. B. Wood, M. Collard, The Human Genus. *Science,* **284**, 65-71 (1999).
23. A. D. Sylvester, Locomotor decoupling and the origin of hominin bipedalism. *Journal of Theoretical Biology*, **242**, 581-590 (2006).

24. L. R. Berger, D. J. de Ruiter, S. E. Churchill, P. Schmid, K. J. Carlson, P. H. G. M. Dirks, J. M. Kibii, *Australopithecus sediba*: A New Species of *Homo*-Like Australopith from South Africa. *Science,* **328 (5975)**, 195-204 (2010).

25. P. Brown, T. Sutikna, M. J. Morwood, R. P. Soejono, Jatmiko, E. Wayhu Saptomo, R. Awe Due, A new small-bodied hominin from the Late Pleistocene of Flores, Indonesia. *Nature*, 431, pp. 1055-1061 (2004).

26. L. R Berger, J. Hawks, D. J. de Ruiter, S. E. Churchill, P. Schmid, L. K. Delezene, T. L. Kivell, H. M. Garvin, S. A. Williams, J. M. DeSilva, M.M. Skinner, C. M. Musiba, N. Cameron, T. W. Holliday, W. Harcourt-Smith, R. R. Ackermann, M. Bastir, B. Bogin, D. Bolter, J. Brophy, Z. D. Cofran, K. A. Congdon, A. S. Deane, M. Dembo, M. Drapeau, M. C. Elliot, E. M. Feuerriegel, D. Garcia-Martinez, D. J. Green, A. Gurtov, J. D. Irish, A. Kruger, M. F. Laird, D. Marchi, M. R. Meyer, S. Nalla, E. W. Negash, C. M. Orr, D. Radovic, L. Schroeder, J. E. Scott, Z. Throckmorton, M. W. Tocheri, C. VanSickle, C. S. Walker, P. Wei, B. Zipfel, *Homo naledi*, a new species of the genus *Homo* from the Dinaledi Chamber, South Africa. *eLife* 4:e09560 (2015).

27. M. M. Barak, D. E. Lieberman, D. Raichlen, H. Pontzer, A. G. Warrener, J-J. Hublin, Trabecular Evidence for a Human-Like Gait in *Australopithecus africanus*. *PLoS ONE*, **8**, e77687 (2013).

28. M. M. Skinner, N. B. Stephens, Z. J. Tsegai, A. C. Foote, N. H. Nguyen, T. Gross, D. H. Pahr, J-J Hublin, T. L. Kivell, Human-like hand use in *Australopithecus africanus*. *Science*, **347**, 395-399 (2015).

29. T. M. Ryan, K. J. Carlson, A. D. Gordon, N. Jablonski, C. N. Shaw, J. T. Stock, Human-like hip joint loading in *Australopithecus africanus* and *Paranthropus robustus*. *Journal of Human Evolution*, **121**, 12-24 (2018).

30. L. Georgiou, T. L. Kivell, D. H. Pahr, L. T. Buck, M. M. Skinner, Trabecular architecture of the great ape and human femoral head. *Journal of Anatomy*, doi:10.1111/joa.12957 (2019).
31. J.P.P. Saers, Y. Cazorla-Bak, C.N. Shaw, J.T. Stock, T.M. Ryan, Trabecular bone structural variation throughout the human lower limb. *Journal of Human Evolution*, **97**, 97-108 (2016).
32. M. M. Barak, D. E. Lieberman, J-J. Hublin, A Wolff in sheep's clothing: trabecular bone adaptation in response to changes in joint loading orientation. *Bone*, **49**, 1141-1151 (2011).
33. T. M. Ryan, C. N. Shaw, Unique suites of trabecular bone features characterize locomotor behavior in human and non-human anthropoid primates. *PLoS ONE*, **7**, e41037 (2012).
34. C. J. Dunmore, T. L. Kivell, A. Bardo, M. M. Skinner, Metacarpal trabecular bone varies with distinct hand-positions used in hominid locomotion. *Journal of Anatomy*, doi:10.1111/joa.12966 (2019).
35. A. I. R. Herries, J. Shaw, Palaeomagnetic analysis of the Sterkfontein palaeocave deposits: implications for the age of the hominin fossils and stone tool industries. *Journal of Human Evolution*, **60**, 523-539 (2011).
36. K. Reed, J. Fleagle, R. Leakey, *The Paleobiology of Australopithecus. Vertebrate Paleobiology and Paleoanthropology*. Dordrecht: Springer (2013).
37. K. Kuman, R. J. Clarke, Stratigraphy, artefact industries and hominid associations for Sterkfontein, Member 5. *Journal of Human Evolution*, **38**, 827-847 (2000).
38. D. E. Granger, R. J. Gibbon, K. Kuman, R. J. Clarke, L. Bruxelles, M. W. Caffee, New cosmogenic burial ages for Sterkfontein Member 2 *Australopithecus* and Member 5 Oldowan", *Nature*, **522**, 85 (2015).

547 39. K. Isler, 3D-Kinematics of vertical climbing in hominoids. *American Journal of*
548 *Physical Anthropology*, **126**, 66–81 (2005).
549 40. E. M. Finestone, M. H. Brown, S. R. Ross, H. Pontzer, Great ape walking kinematics:
550 Implications for hominoid evolution. *American Journal of Physical Anthropology*
551 **166**, 43-55 (2018).
552 41. S. K. S. Thorpe, R. H. Crompton, Orangutan positional behavior and the nature of
553 arboreal locomotion in Hominoidea. *American Journal of Physical Anthropology*,
554 **131**, 384-401 (2006).
555 42. H. Yoshida, A. Faust, J. Wilckens, M. Kitagawa, J. Fetto, E. Y. Chao, Three-
556 dimensional dynamic hip contact area and pressure distribution during activities of
557 daily living. *Journal of Biomechanics*, **39**, 1996-2004 (2006).
558 43. S. J. Abbass, G. Abdulrahman, Kinematic analysis of human gait cycle. *Nahrain*
559 *University College of Engineering Journal (NUCEJ)*, **16**, 208-222 (2014).
560 44. D. J. Green, H. Chirchir, E. Mbua, J. W. K. Harris, D. R. Braun, N. L. Griffin, B. G.
561 Richmond, Scapular anatomy of *Paranthropus boisei* from Ileret, Kenya. *Journal of*
562 *Human Evolution*, **125**, 181-192 (2018).
563 45. M. J. Remis, Tree structure and sex differences in arboreality among western lowland
564 gorillas (*Gorilla gorilla gorilla*) at Bai Hokou, Central African Republic. *Primates*,
565 **40**, 383-396 (1999).
566 46. G. Giarmatzis, I. Jonkers, M. Wesseling, S. Van Rossom, S. Verschueren, Loading of
567 hip measured by hip contact forces at different speeds of walking and running.
568 *Journal of Bone and Mineral Research,* **30**, 1431-1440 (2015).
569 47. S. C. Reynolds, J. M. Kibii, Sterkfontein at 75: review of paleoenvironments, fauna,
570 dating and archaeology from the hominin site of Sterkfontein (Gauteng Province,
571 South Africa). *Palaeontologia Africana*, **55**, 59-88 (2011).

572 48. I. Singh, Squatting facets on the talus and tibia in Indians. *Journal of Anatomy*, **93**,
573 540-550 (1959).
574 49. M. R. Lague, H. Chirchir, D. J. Green, E. Mbua, J. W.K. Harris, D. R. Braun, N. L.
575 Griffin, B. G. Richmond, Cross-sectional properties of the humeral diaphysis of
576 *Paranthropus boisei*: Implications for upper limb function. *Journal of Human*
577 *Evolution*, **126**, 51-70 (2019).
578 50. M. Domínguez-Rodrigo, T. R. Pickering, E. Baquedano, A. Mabulla, D. F. Mark, C.
579 Musiba, H. T. Bunn, D. Uribelarrea, V. Smith, F. Diez-Martin, A. Pérez-González, P.
580 Sánchez, M. Santonja, D. Barboni, A. Gidna, G.Ashley, J. Yravedra, J. L. Heaton, M.
581 C. Arriaza, First partial skeleton of a 1.34-million-year-old *Paranthropus boisei* from
582 Bed II, Olduvai Gorge, Tanzania. *PlosOne*, doi: 10.1371/journal.pone.0080347
583 (2013).
584 51. P. S. Ungar, M. Sponheimer, The diets of early hominins. *Science*, **334 (6053)**, 190-
585 193 (2011).
586 52. Y. Haile-Selassie, B. Z. Saylor, A. Deino, N. E. Levin, M. Alene, B. M. Latimer, A
587 new hominin foot from Ethiopia shows multiple Pliocene bipedal adaptations. *Nature*,
588 **483**, 565-569 (2012).
589 53. H. Scherf, R. Tilgner, A new high-resolution computed tomography (CT)
590 segmentation method for trabecular bone architectural analysis. *American Journal of*
591 *Physical Anthropology*, **140**, 39-51 (2009).
592 54. C. J. Dunmore, G. Wollny, M. M. Skinner, MIA-Clustering: a novel method for
593 segmentation of paleontological material. *PeerJ*, **6**, e4374 (2018).
594 55. T. Gross, T. L. Kivell, M. M. Skinner, N. H. Nguyen, D. H. Pahr, A CT-image-based
595 framework for the holistic analysis of cortical and trabecular bone morphology.
596 *Palaeontologia Electronica*, **17**, 1-13 (2014).

56. J. Ahrens, B. Geveci, C. Law, 'ParaView: An end-user tool for large data visualization', in C. D. Hansen, C. R. Johnson (eds). *Visualization handbook.* Burlington, MA: Butterworth- Heinemann, 717-731 (2005).
57. R Development Core Team. R: A language and environment for statistical computing. Vienna, Austria: The R Foundation for Statistical Computing (2017).
58. P. Cignoni, M. Corsini, G. Ranzuglia, Meshlab: an open-source 3d mesh processing system. *ERCIM News*, **73**, 45-46 (2008).
59. P. Gunz, P. Mitteroecker, Semilandmarks: a method for quantifying curves and surfaces. *Hystrix, the Italian Journal of Mammalogy*, **24**, 103-109 (2013).
60. S. Schlager, 'Morpho and Rvcg – Shape Analysis in R', in G. Zheng, S. Li, G. Szekely (eds.). *Statistical Shape and Deformation Analysis*. Academic Press, 217-256 (2017).

Figure 1. A schematic of hypothesized femoral head pressure and trabecular bone distribution at various flexion angles. (A) Hypothesized areas of high (pink) and low (yellow) pressure on the femoral head, based on how the femoral head fits within the incongruent hip joint at low flexion (e.g, bipedalism: above) and moderate to high flexion (e.g. during terrestrial quadrupedalism and vertical climbing; below). (B) the predicted resulting areas of high bone volume fraction (BV/TV). For a more detailed explanation refer to Supporting Figure 4.

Figure 2. Non-human great ape hip flexion angles during terrestrial vertical climbing and quadrupedalism, and BV/TV distribution in the femoral head. (A) Great ape hip posture in maximum flexion (~55^{o}-60^{o}) during climbing[39], as well as joint posture at toe-off

(~110^{o}) during terrestrial knuckle-walking[40]. Brackets indicate regions of presumed high pressure during large flexion (red - anterior) and slight flexion (blue - posterior). (B) Superior view of BV/TV distribution in the femoral head of *Pongo, Gorilla* and *Pan*. High BV/TV is indicated in red and low BV/TV in blue. Note the two distinctly high BV/TV concentrations in *Gorilla* and the expansive distribution in *Pongo*, with *Pan* exhibiting an intermediate pattern. (C) Distribution of highest BV/TV values within the femoral head of *Pongo, Gorilla* and *Pan*. Internal concentrations are visualised for BV/TV above the 80th percentile. This threshold was chosen to visualise the regions where the highest BV/TV is found within each specimen. Note that the internal high BV/TV forms an inverted cone in *Pongo,* and two convergent pillars in *Pan* and *Gorilla*.

Figure 3. Human hip flexion angles during bipedal locomotion and BV/TV distribution in the femoral head of *Homo sapiens*. (A) Modern human hip posture during bipedal walking at heel-strike (~160^{o}) and toe-off (~175^{o}), when ground reaction force is highest. Blue brackets indicate regions of inferred high pressure during bipedal walking. (B) Superior view of BV/TV distribution in the femoral head in fossil and recent *H. sapiens* is consistent with this loading prediction. High BV/TV is indicated in red and low BV/TV in blue. (C) Distribution of highest BV/TV values within the femoral head of *Homo sapiens*. Internal concentrations are visualised for BV/TV above the 80th percentile. This threshold was chosen to visualise the regions where the highest BV/TV is found within each specimen. Note that the internal high BV/TV forms one pillar in *Homo*.

Figure 4. BV/TV distribution in the subchondral layer of the femoral head (A) and within the femoral head (B) in the extant and fossil taxa. StW 311 resembles the non-human ape-like patterns, while StW 522 resembles the human pattern. Internal concentrations

are visualised for BV/TV above the 80th percentile. This threshold was chosen to visualise the regions where the highest BV/TV is found within each specimen. Specimens are scaled to their own data range.

Figure 5. PCA of the relative BV/TV distribution in the femoral head. 2D plot showing in red the landmarks that have the highest loading on each axis. RBV/TV values in landmarks on the inferior aspect of the head have the highest positive loading on PC1, (separating *H. sapiens* from the non-human apes) and RBV/TV values in landmarks on two regions across the superior aspect of the head have the highest negative loading (being most clearly expressed in *Gorilla*). PC2 does not separate taxa but is driven by high RBV/TV posteriorly versus anterosuperiorly. Considerable variation, specifically in *Gorilla*, could relate to sexual dimorphism and differences in habitual hip angles between the sexes.

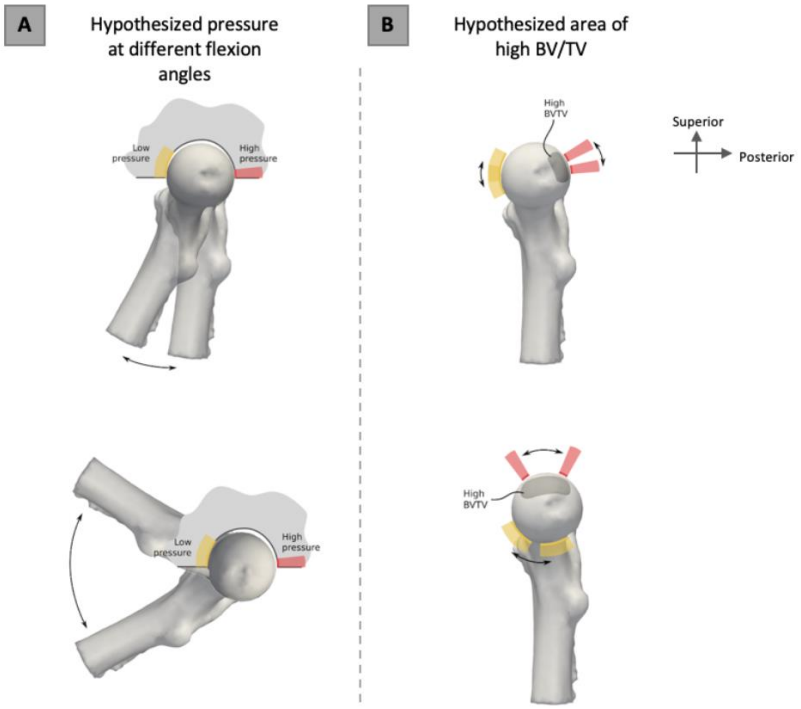
A
Hypothesized pressure at different flexion angles
Low pressure
High pressure
Low pressure
High pressure
B
Hypothesized area of high BV/TV
High BVTV
High BVTV
Superior
Posterior

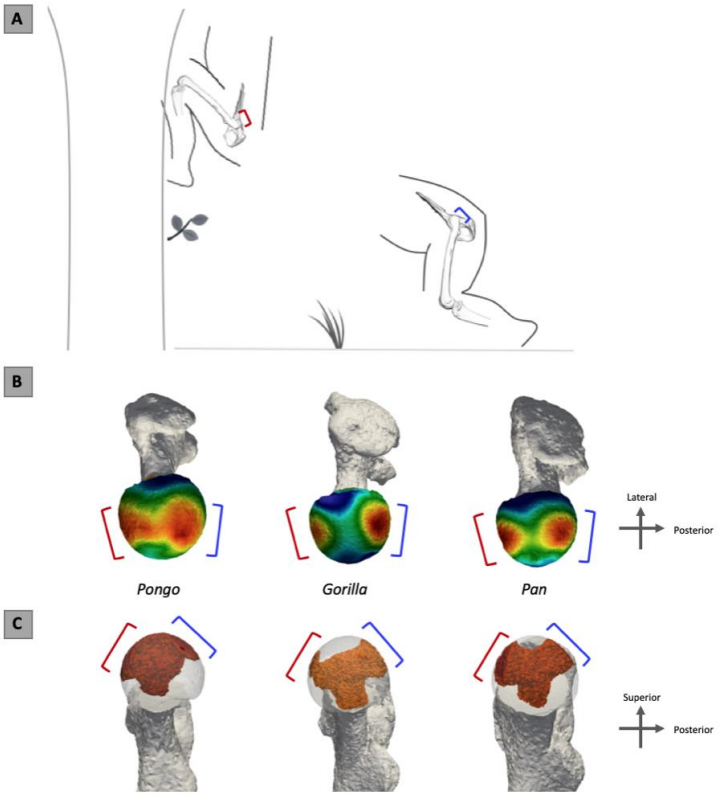
A
B
Lateral
Posterior
Pongo
Gorilla
Pan
C
Superior
Posterior

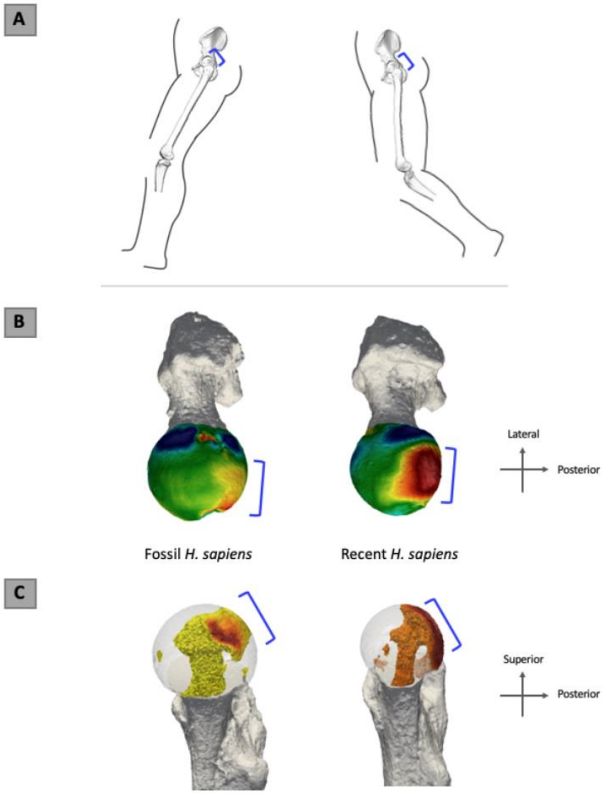
A
B
Lateral
Posterior
Fossil H. sapiens
Recent H. sapiens
C
Superior
Posterior

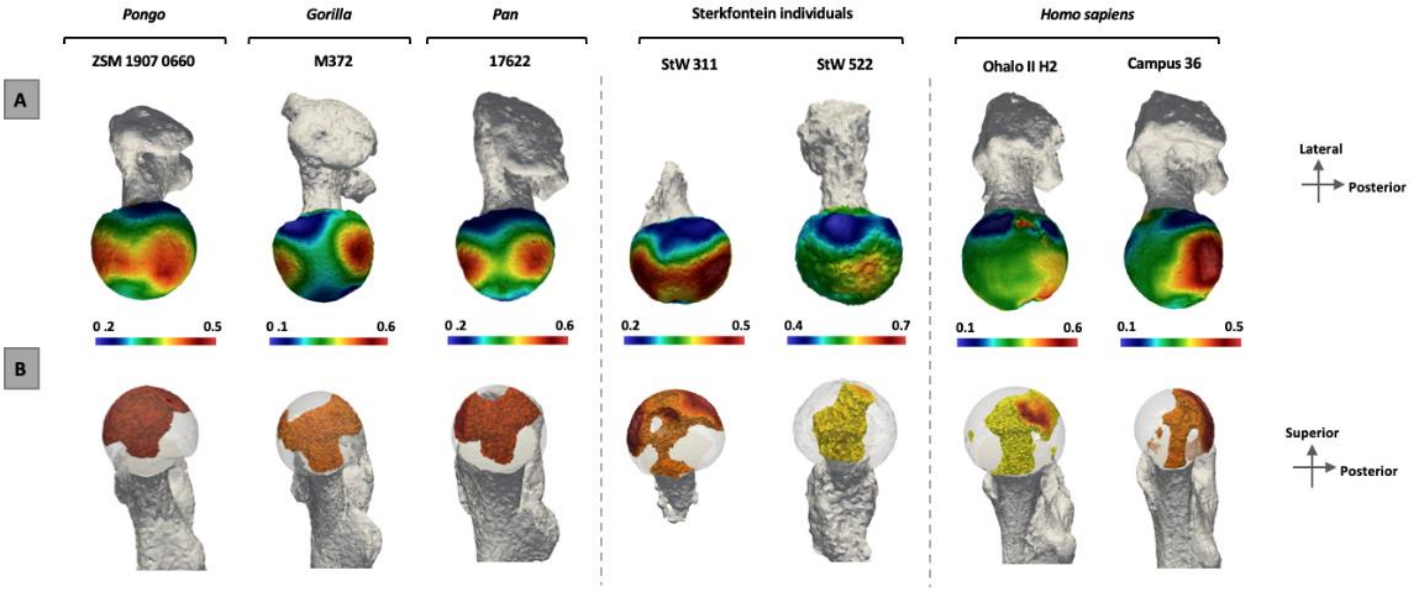
Pongo
Gorilla
Pan
Sterkfontein individuals
Homo sapiens
ZSM 1907 0660
M372
17622
StW 311
StW 522
Ohalo II H2
Campus 36
A
B
0 .2
0.5
0 .1
0.6
0 .2
0.6
0.2
0.5
0.4
0.7
0.1
0.6
0.1
0.5
Lateral
Posterior
Superior
Posterior

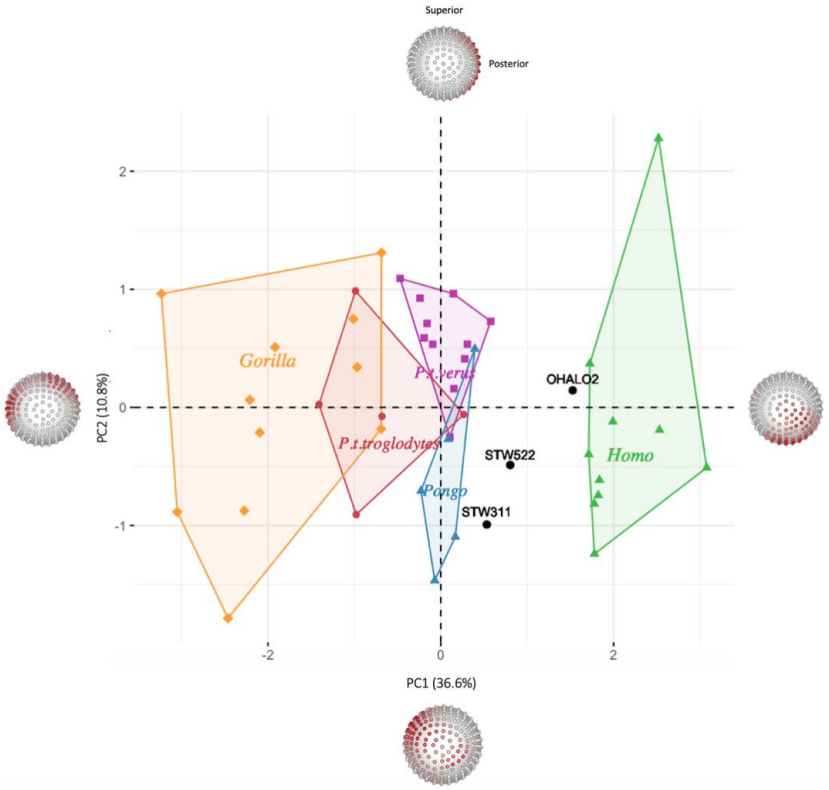
Superior
Posterior
2
1
0
-1
-2
0
2
PC2 (10.8%)
PC1 (36.6%)
Gorilla
P.t.verus
P.t.troglodytes
Pongo
Homo
OHALO2
STW522
STW311